UC San Diego
UC San Diego Previously Published Works

Title

High-molecular-weight linear polymers improve microvascular perfusion after extracorporeal circulation

Permalink

https://escholarship.org/uc/item/0850v62x

Journal

Journal of Applied Physiology, 136(1)

ISSN

8750-7587

Authors

Govender, Krianthan

Walser, Cynthia

Cabrales, Pedro

Publication Date

2024

DOI

10.1152/japplphysiol.00397.2023

Copyright Information

Peer reviewed

RESEARCH ARTICLE

High-molecular-weight linear polymers improve microvascular perfusion after extracorporeal circulation

Krianthan Govender, Cynthia Walser, and Pedro Cabrales

Functional Cardiovascular Engineering Laboratory, University of California San Diego, La Jolla, California, United States

Abstract

High-molecular-weight linear polymers (HMWLPs) have earned the name "drag-reducing polymers" because of their ability to reduce drag in turbulent flows. Recently, these polymers have become popular in bioengineering applications. This study investigated whether the addition of HMWLP in a venoarterial extracorporeal circulation (ECC) model could improve microvascular perfusion and oxygenation. Golden Syrian hamsters were instrumented with a dorsal skinfold window chamber and subjected to ECC using a circuit comprised of a peristaltic pump and a bubble trap. The circuit was primed with lactated Ringer solution (LR) containing either 5 ppm of polyethylene glycol (PEG) with a low molecular weight of 500 kDa (PEG500k) or 5 ppm of PEG with a high molecular weight of 3,500 kDa (PEG3500k). After 90 min of ECC at 15% of the animal's cardiac output, the results showed that the addition of PEG3500k to LR improved microvascular blood flow in arterioles and venules acutely (2 h after ECC), whereas functional capillary density showed improvement up to 24 h after ECC. Similarly, PEG3500k improved venular hemoglobin O_2 saturation on the following day after ECC. The serum and various excised organs all displayed reduced inflammation with the addition of PEG3500k, and several of these organs also had a reduction in markers of damage with the HMWLPs compared to LR alone. These promising results suggest that the addition of small amounts of PEG3500k can help mitigate the loss of microcirculatory function and reduce the inflammatory response from ECC procedures.

NEW & NOTEWORTHY High-molecular-weight linear polymers have gained traction in bioengineering applications. The addition of PEG3500k to lactated Ringer solution (LR) improved microvascular blood flow in arterioles and venules acutely after extracorporeal circulation (ECC) in a hamster model and improved functional capillary density up to 24 h after ECC. PEG3500k improved venular hemoglobin O_2 saturation and oxygen delivery acutely after ECC and reduced inflammation in various organs compared to LR alone.

drag-reducing polymers; extracorporeal circulation; microcirculation; polyethylene glycol; priming fluids

INTRODUCTION

In the mid-1900s, the addition of minute amounts of polymers to Newtonian fluids undergoing turbulent flows showed a reduction in drag, a phenomenon known as the Toms effect (1). These polymers tend to be flexible, linear in molecular structure, and of high molecular weight (MW > 10^6) (2, 3). When added to fluids subjected to turbulence, these polymers stretch along the direction of flow and reduce the drag force exerted on surfaces. As summarized by White and Mungal (4) over a decade ago, there are two main hypotheses that aim to explain why drag reduction occurs. The first hypothesis states that as the extension of these polymers occurs there is an increase in the effective viscosity, leading to a widening of the buffer regime within the turbulent boundary layer, which decreases the frictional forces exerted on surfaces. The second hypothesis states that the elastic energy resulting from elongation of polymer molecules interrupts the cascade of energy from larger to smaller eddies in turbulent flow, causing a widening of the buffer regime, leading to a reduction in drag (5, 6). Irrespective of the

cause of drag reduction, the Toms effect is leveraged today in various engineering applications such as transferring crude oil (7, 8) to reduce the pressure gradient needed in pipelines for higher volumetric flow rates, increasing the transfer efficiency, earning them the name of "drag-reducing polymers" in conventional engineering applications.

Despite turbulent flow regimes seldom appearing within the cardiovascular system, high-molecular-weight linear polymers (HMWLPs) have also branched into the field of intravascular bioengineering applications. Some of the first studies using HMWLP focused on effects within the macrocirculation, primarily with animal models of stenosed major arteries (9) and atherosclerosis (10, 11). However, the benefits of HMWLP are also observable at the microcirculation level, as shown by in vivo experiments exhibiting increased microvascular red blood cell (RBC) perfusion in models of resuscitation from hemorrhagic shock (12) with traumatic brain injury (13, 14), sickle cell disease (15), and ischemia-reperfusion (16, 17). There are several mechanisms that have been investigated to explain the improved microvascular perfusion after the addition of HMWLPs. First, at bifurcation

Correspondence: P. Cabrales (pcabrales@eng.ucsd.edu).

213

points and areas with large changes in vessel cross-sectional area, secondary flows such as eddies and stagnation points can occur. The addition of HMWLPs ex vivo has shown altered flow conditions by which these secondary flows start to manifest, with the changes becoming more pronounced as the scale of the flow regime decreases (18), which can affect the pressure drop between major arteries and arterioles in the microvascular bed (19). Second, both ex vivo and in vivo tests have shown that the addition of HMWLPs in microvascular networks tends to decrease the cell-free layer (CFL) (20, 21), which is a hemodynamic region situated between the membrane of vascular endothelial cells and the RBC core where there is minimal RBC traffic (22). The reduction in CFL thickness leads to reduced plasma skimming from parent to daughter branches, causing an increase in hematocrit and viscosity in daughter branches, ultimately leading to increased capillary perfusion. Another effect of decreased CFL is an increase in the wall shear stress (WSS) (23), which promotes mechanotransduction within vascular endothelial cells. Vascular mechanotransduction leads to the secretion of vasodilatory products, such as prostaglandins and nitric oxide (NO), ultimately causing relaxation of smooth muscle, vasodilation, increased blood flow, and reduced vascular resistance (24).

The present study aims to extend the application of HMWLPs to address the reduced microcirculatory flow that results from extracorporeal circulation (ECC) procedures. ECC procedures are any procedures that involve blood circulation outside the body and encompass procedures such as hemodialysis, cardiopulmonary bypass (CPB), and extracorporeal membrane oxygenation (ECMO) (25). We have previously shown that microcirculatory flow is impaired in a model of ECC procedures, with minimal recovery at 24 h after ECC, even when using an isooncotic priming fluid (26). Therefore, we hypothesize that the addition of HMWLP to ECC priming fluids can help preserve microcirculation perfusion and support microvascular oxygen delivery and extraction. We utilize a small-animal model instrumented with a dorsal window chamber to examine the microcirculation with intravital microscopy, coupled with a scaled-down ECC circuit representing the flow direction utilized in venoarterial extracorporeal membrane oxygenation (VA-ECMO), allowing for in vivo assessment of microvascular hemodynamics and oxygenation.

MATERIALS AND METHODS

The study was broken up into in vitro and in vivo experiments. The purpose of the in vitro experiments was to characterize the circuit and to determine any changes in hemolysis. The in vivo experiments were utilized to determine the changes in microcirculation perfusion and oxygenation.

For the ex vivo recirculation runs, three donor animals were used for each of the three groups. For the in vivo ECC experiments, six animals were used for the polyethylene glycol (PEG)500k (molecular weight of 500 kDa) group and six animals were used for the PEG3500k (molecular weight of 3,500 kDa) group. Since the lactated Ringer solution (LR) control had already been performed in the previous study (26), two additional experiments with LR were conducted. Four animals were randomly selected from the previous data

set and combined with the two new experiments to define a new set of six control animals for this study.

Preparation of High-Molecular-Weight Linear Polymer Solutions

Two polyethylene glycol (PEG) solutions with different molecular weights but same mass concentrations were tested: PEG500k and PEG3500k. Fifty parts per million (ppm) of PEG 500 kDa polymers (Fujifilm Wako Chemicals, Osaka, Japan) was made by mixing 0.005 g in 100 mL of saline into a beaker with a stir rod situated on a magnetic plate. The solution was allowed to mix for at least 4 h and was observed for any visible clumps to ensure that the polymers were dissolved. Lactated Ringer solution (LR) was then added to the 50 ppm PEG-saline solution in a 9-to-1 ratio, resulting in a 5 ppm solution of PEG 500 kDa in LR (PEG500k). The PEG500k solution served as a control to account for the addition of PEG to the priming fluid. The PEG 3,500 kDa solution was made with a similar method, by dissolving 0.0035 g in 100 mL of saline and then further diluting in LR in a 6-to-1 ratio, resulting in a 5 ppm solution of PEG 3,500 kDa in LR (PEG3500k). Solutions were made weekly and stored at 4°C. Before use in any experiments, vials were placed on a tube rotator for a minimum of 1 h before being used.

Benchtop Circuit Testing

To evaluate the circuit, benchtop testing was performed. Four milliliters of blood was drawn from anesthetized donor Golden Syrian hamsters via cardiac puncture with a 22-gauge needle and syringe; 50 IU heparin/mL of whole blood was added, and 4 mL was separated out into a vial. The remaining blood was placed on a vial rotator until the end of the experiment.

The circuit was primed with LR, the PEG500k solution, or the PEG3500k solution. The circuit, consisting of a peristaltic pump, tubing (0.152-cm diameter), and a bubble trap, was then connected to the vial. The pump was ramped up for 15 min, run at 2 mLPM for 60 min, and then ramped down for 15 min. Samples were taken at 0 min, 15 min, 45 min, 75 min, and 90 min during the run via the vent line in the bubble trap; 50 μL was analyzed for hematocrit (Hct) and plasma hemoglobin (pHb) with a centrifuge, and 80 μL was used for analysis with a blood gas analyzer. At the end of the experiment, both blood samples before ECC and after 90 min of ECC were centrifuged and plasma stored for analysis of coagulation and inflammatory markers.

Animal Preparations

Male Golden Syrian hamsters were purchased from Charles River Laboratory (Wilmington, MA). The hamsters were housed in a 12:12-h light-dark cycle and allowed free access to water and Teklad 8604 rodent diet (Envigo, Indianapolis, IN). Animals were cared for in accordance with the NIH *Guide for the Care and Use of Laboratory Animals*, and all experiments performed were approved by the University of California, San Diego (UC San Diego) Institutional Animal Care and Use Committee (IACUC). Animals weighing 60–75 g were then instrumented with a dorsal window chamber under ketamine-xylazine anesthetic, as previously described (26). Briefly, the hamsters' hair was removed on their dorsal side and the skin

stretched. The topmost layer of skin and adipose tissue was removed to reveal the underlying vasculature. The preparation was then covered with a thin layer of saline, a glass coverslip was applied, and the skin was sutured to two ends of a titanium frame. Animals were allowed to recover for a minimum of 24 h before being instrumented with an arterial catheter (PE50 with PE10 tip) in the carotid artery and tunneled rostral to the window chamber on the dorsal side of the animal under ketamine-xylazine anesthetic. The catheter was filled with 30 IU heparin/mL saline solution to preserve patency. Animals were allowed to recover for a minimum of 24 h before the start of the experiment. Animals were placed in an acrylic tube, and measurements were taken in the awake (unanesthetized) state, as shown in Fig. 1. After the experiment, blood samples were taken and the animals were euthanized with an overdose of pentobarbital sodium (300 mg/kg Euthasol; Virbac AH Inc., Carros, France) administered into the exteriorized arterial catheter. The spleen, kidney, liver, heart, lung, and urine (if present) were then taken for analysis.

Baseline Acceptance Criteria

Baseline values were assessed to determine whether animals were acceptable for the study. Window chambers were analyzed at the microscope with a ×40 water immersion lens objective, and chambers that had limited visibility, excessive inflammation, or edema were not used for experiments. After the chambers were analyzed for clarity, the hamsters were weighed and the following systemic parameters were then analyzed: *1*) $100 <$ mean arterial pressure (MAP, mmHg) < 130; *2*) $400 <$ heart rate (HR, beats/min) < 500; *3*) Hct $> 40\%$. After each animal passed the acceptance criteria, baseline (BL) measurements were taken.

Extracorporeal Circulation

After BL measurement were taken, the animals were subjected to extracorporeal circulation (ECC), as described previously (26). Animals were anesthetized with a vaporizer with isoflurane at 2.5% mixed with room air. Eye lubricant

was applied to the animal before it was placed supine on a surgical board. The neck was disinfected, and the soft tissue was dissected until the jugular vein was isolated. The vessel was ligated rostrally and clamped caudally, and a small incision was made into the vessel. A 3 Fr polyurethane (PU) catheter with three distal fenestrations was then inserted to a depth of ∼2 cm into the vessel, and backflow of blood was verified. A bolus of heparin (0.05 IU/g animal wt) was administered via the carotid arterial catheter, and the isoflurane was turned down to 1.25%. After the circuit was primed with LR, the PEG500k solution, or the PEG3500k solution, the animal was connected to the same circuit as the one used for the ex vivo blood recirculation tests by connecting the jugular catheter to the circuit inflow and the carotid catheter to the circuit outflow. The animal was then covered with a heating blanket connected to a water recirculation pump set at 37°C to help maintain normothermia. The circuit was ramped up for 15 min, held for 60 min at a flow rate equivalent to 15% of the animal's cardiac output (CO), and then ramped down for 15 min. To scale the circuit flow rate based on hamster weight, the CO was estimated using the cardiac index of Golden Syrian hamsters from previously published data obtained with thermodilution techniques (27). The animal was then disconnected from the circuit, and the circuit was drained of blood to analyze plasma. The jugular catheter was removed, and the carotid catheter was flushed with heparinized saline (30 IU/mL) to preserve patency. The jugular and neck were sutured shut, and a cauterizer was used to help prevent bleeding. Buprenorphine (0.02 mL) and saline (1 mL) were subcutaneously injected as an analgesic and to help with fluid loss, respectively. The animal was removed from the isoflurane anesthesia and placed in a cage situated on a heated blanket. The animal was allowed a minimum of 30 min inside the cage with wet food to recuperate before subsequent measurements were taken 1 h, 2 h, and 24 h after ECC.

Systemic Parameters

The arterial catheter was utilized to measure systemic parameters. Mean arterial pressure (MAP) was measured by fitting the catheter's distal end to a Meritrans DTXPlus differential pressure transducer (Merit Medical, South Jordan, UT), which was connected to a MP150 data acquisition system (BIOPAC Systems Inc, Goleta, CA). The pressure signal was analyzed with AcqKnowledge software version 3.7 (BIOPAC Systems Inc) to calculate heart rate (HR). Blood samples were taken and analyzed as described in *Benchtop Circuit Testing*. Bicarbonate concentration was calculated with the Henderson–Hasselbalch equation, pH, and arterial partial pressure of carbon dioxide (P_{CO_2}).

Microcirculation Measurements

The implanted dorsal skinfold window chamber was used to measure changes in hemodynamics at various time points with intravital microscopy techniques. Each chamber was first mapped, identifying at least five arterioles and five venules. Functional capillary density (FCD) was then assessed by counting the number of capillaries perfused with red blood cells (RBCs) along two lines of the window chamber. The diameter and velocity of arterioles and venules were then measured with techniques previously described (28,
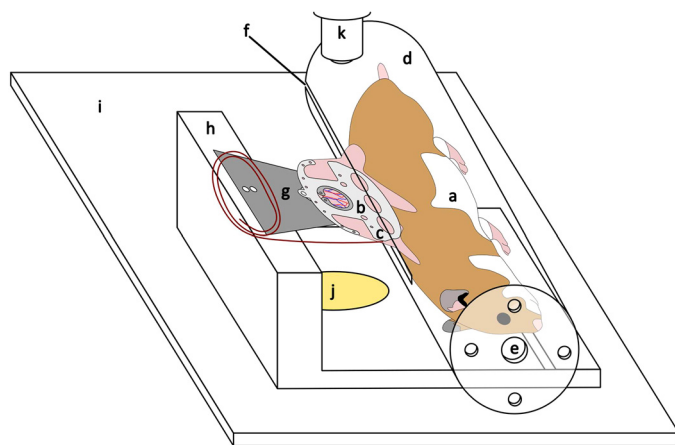
Figure 1. Schematic of intravital microscopy for microvascular measurements in the awake, unanesthetized state. *a*, male Golden Syrian hamster; *b*, dorsal skinfold window chamber; *c*, exteriorized arterial line; *d*, acrylic tube; *e*, breathing holes; *f*, slit for the window chamber; *g*, fixation plate; *h*, acrylic stage; *i*, microscope mechanical stage; *j*, light source; *k*, water immersion ×40 lens objective.

29). To measure velocity, a two-slit photometric technique coupled with a correlogram was utilized. As light shines through the vessel, the shadows of RBCs passing through are captured by each photodiode. The correlogram calculates the phase shift between the two signals and outputs a voltage corresponding to the velocity. To measure diameter, the microscope was connected to a camera, a closed-circuit television, and an image shearing module. The image of each vessel was sheared, with the distance corresponding to a known value in micrometers. Flow rate ($\dot{Q}$) within each vessel was calculated from velocity (v) and diameter (d) (30):

$$\dot{Q} = \left(\frac{d^2}{4}\right)\left(\frac{v}{1.6}\right).$$

Hyperspectral Imaging

Hemoglobin oxygen saturation (So_2) within individual arterioles and venules was assessed by hyperspectral imaging, as described previously (26, 31). A segment of the window chamber was imaged with a Pika-L hyperspectral camera (Resonon, Bozeman, MT). The image was then preprocessed by first truncating the spectral range of the image and applying a mean and Savitsky–Golay filter. A mask was applied to isolate vessels, and areas within each vessel were then selected. The absorbance values within the vessels were compared to reference spectra for hamster deoxyhemoglobin and oxyhemoglobin.

Hyperspectral images were taken at each time point for each animal within each group, resulting in a total of 72 images taken for this study. The images were taken after a minimum of 10 min after positioning the hamster underneath the hyperspectral camera, providing time to adjust to the change in environment. The images were postprocessed to assess So_2 within arterioles and venules. Microcirculatory fields were evaluated for clarity of the vasculature before manual selection for arteriole or venule So_2. To obtain representative images, average values for each BL image shown were compared to average values at BL for each experimental group. Each image contained at least four selected areas within vessels at BL to be included for analysis.

Statistical Analysis

Once all experimental data was gathered, statistical analysis was performed in RStudio using R version 4.0.3. Sample size was determined based on $\alpha = 0.05$ and a statistical power of 0.9. Velocity, diameter, flow, and FCD measurements were all normalized to BL to remove any variability between vessels. Extreme values were identified ($3 \times$ interquartile range) and removed from the data before statistical tests were applied. Data was assessed for normality with the Shapiro-Wilk test and subsequently analyzed with Tukey's range test and presented as box-and-whisker plots, as bar plots for mean and standard deviation, or in tabular form.

RESULTS

Ex Vivo Benchtop Testing

Supplemental Table S1 displays the changes in hematological parameters over the 90 min of blood recirculation. Glucose and lactate showed no significant difference between groups at any time point. Glucose levels showed an expected downward trend over time since blood cells utilize glucose as an energy source. Lactate levels increased at 15 min, which is likely due to the presence of lactate within the LR used. Sodium and potassium remained stable over the duration of ECC. Chloride displayed an upward trend whereas calcium and pH showed a downward trend during 90 min of recirculation. It should be noted that before the start of recirculation there was statistical significance in pH and chloride between LR and PEG3500k and LR and PEG500k, respectively. Hemoglobin was also tracked over time during the ECC runs. Total hemoglobin (tHb) and Hct showed a significant decrease after 15 min for all three groups, which most likely resulted from the priming fluid diluting the blood in the circuit. The only statistical significance observed between groups occurred at 90 min of ECC, when Hct was significantly lower in the LR group compared with the PEG500k group. Plasma hemoglobin (pHb) was used as a measure of hemolysis and showed an increase over the 90 min of ECC; both LR and PEG500k showed significantly higher pHb levels after 45 min of recirculation time compared with before ECC.

Serum inflammatory and coagulation markers were evaluated in plasma samples taken before and after 90 min of ex vivo blood recirculation (Supplemental Table S2). Before ECC, interleukin-6 (IL-6) and interleukin-10 (IL-10) levels showed no significance between any of the groups. However, IL-6 and IL-10 statistically increased for all groups 90 min after ECC. This increase is drastic, considering that the circuit itself contained priming fluid, which effectively dilutes the blood circulating through the system. This dilution effect may partially explain the trend observed in coagulation markers, which exhibited a significant decrease between pre-ECC and post-ECC time points. Fibrinogen, soluble glycoprotein V, and platelet factor 4 all showed no significance between any groups before ECC; the only marker that showed statistical significance between groups before ECC was P-selectin. After 90 min of ECC, LR and PEG3500k groups were statistically lower compared with the PEG500k group for all four coagulation markers.
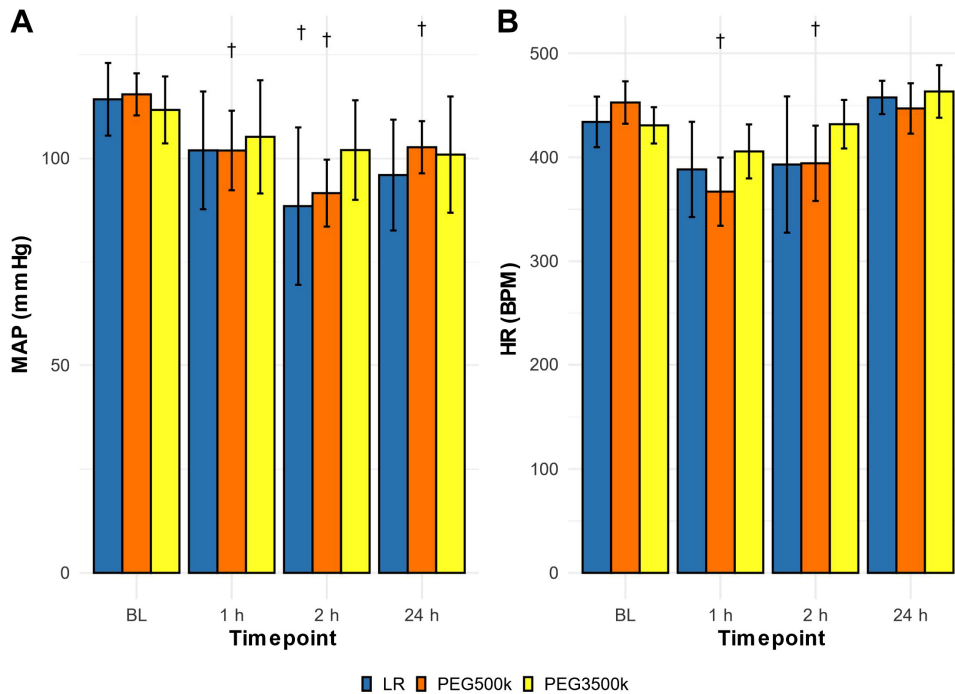
In Vivo ECC

Systemic parameters.
Mean arterial pressure (MAP) and heart rate (HR) displayed no significance between groups at any time point (Fig. 2). Both MAP and HR showed a decrease immediately following ECC, with LR and PEG500K showing a significant decrease in MAP at 2 h after ECC. The only statistically significant change observed in HR was in the PEG500k group at 1 and 2 h after ECC, compared to BL levels.

Electrolytes and hematology.
The electrolyte and hematology results from the in vivo arterial blood samples are shown in Table 1. Hct and tHb declined at all post-ECC time points, and by 2 h all three groups were significantly lower compared to BL levels. pHb increased after ECC for both the LR and PEG3500k groups but did not change for the PEG500k group. Interestingly, pHb in the PEG3500k group was significantly elevated compared to the LR group at both 1 and 2 h after ECC. At 24 h, the pHb for all three groups was back to BL levels. Arterial So_2 for all three groups was significantly elevated at 1 and 2 h after ECC. Arterial So_2 for LR was significantly higher than that for PEG3500k at 1 h after ECC and significantly higher

Figure 2. Systemic parameters from in vivo experiments, with mean arterial pressure (MAP; *A*) and heart rate (HR; *B*). BPM, beats/minute. Bar plot displays means and SD. $N = 6$ hamsters for all groups. $†P < 0.05$ compared to baseline (BL), within each group. LR, lactated Ringer solution; PEG500k, polyethylene glycol (PEG) 500 kDa in LR; PEG3500k, PEG 3,500 kDa in LR.

than that for PEG500k at 2 h after ECC. At 24 h, only the PEG3500k group showed elevated arterial So_2 compared to BL. Arterial partial pressure of carbon dioxide (Pco_2) was significantly lower in all three groups at 2 h after ECC but recovered back to BL levels by 24 h after ECC. Arterial partial pressure of oxygen (Po_2) increased at 1 and 2 h after ECC for all three groups compared to BL. Additionally, Po_2 for LR was significantly higher than that for both PEG500k and PEG3500k at 1 and 2 h after ECC. Whereas Po_2 levels for LR and PEG500k were able to return to BL levels at 24 h after ECC, PEG3500k remained significantly elevated. Electrolytes and pH showed acute changes after ECC but were able to return to BL levels at 24 h after ECC. Potassium levels for both LR and PEG500k were significantly lower than BL at both 1 and 2 h after ECC. On the other hand, chloride levels for all three groups were significantly increased at both 1 and 2 h compared to BL. Bicarbonate was calculated with the Henderson–Hasselbalch equation and showed a significant decrease from BL at 1 and 2 h in all three groups. The results also show that the bicarbonate level for PEG3500k was statistically higher compared to LR at both 1 and 2 h after ECC. Calcium and sodium showed minimal change after ECC. pH did not show any significance between groups but displayed a significant decrease from BL at 1 and 2 h for both PEG500k and PEG3500k groups. Lactate levels were lower in the PEG3500k group compared to LR at both 1 and 2 h after ECC.

Arteriole and venule perfusion.

Figure 3, *left*, displays the changes in arteriole perfusion within the window chamber. There were no significant differences in arteriole diameter at any post-ECC time point between groups. PEG3500k was the only group to show no change in arteriole diameter at all post-ECC time points. Most of the differences between groups were observed in velocity, where the PEG3500k group displayed a significantly higher arteriole velocity compared to the other two groups at

1 and 2 h after ECC. Additionally, although all three groups showed a significant decrease in arteriole velocity from BL to 1 h after ECC, the PEG3500k group was the only group able to recover back to BL at 2 h after ECC. Overall, arteriole blood flow at both 1 and 2 h after ECC in the PEG3500k group was significantly higher compared to the LR and PEG500k groups. At 24 h after ECC, the PEG3500k group displayed elevated arteriole blood flow compared to the LR control group, with no statistical significance between the PEG500k group and the LR control group.

Venule perfusion is shown in Fig. 3, *right*. Venule diameter at all post-ECC time points was significantly elevated in the PEG500k group compared to the PEG3500k group. At 24 h, all three groups displayed significant differences, with PEG500k being the largest, followed by PEG3500k and the LR control. The LR control was the only group to show a significant decrease in venule diameter, which occurred at 24 h. Venule velocity was significantly elevated in the PEG3500k group compared to both other groups at 1 and 2 h after ECC. At 2 h after ECC, the PEG3500k group was the only group to recover back to BL levels. Venule blood flow was significantly increased in the PEG3500k group compared to both other groups at 2 h after ECC. The LR control and PEG3500k groups showed significantly decreased venule blood flow at both 1 and 2 h after ECC compared to BL levels. At 24 h, the PEG3500k was able to recover back to BL values, whereas the PEG500k group displayed significantly higher venule flow.

Distribution of hemoglobin oxygen saturation.

Hemoglobin oxygen saturation (Fig. 4) within the microcirculation (Fig. 5) showed significance between groups at baseline for both arterioles and venules. Arteriole So_2 (Sa_{O_2}) was significantly lower in the PEG500k group compared to both the LR and PEG3500k groups at BL, 1 h after ECC, and 24 h after ECC. Minimal changes were observed in Sa_{O_2} compared

Table 1. *Changes in hematology and blood gases from arterial samples from in vivo experiments*

	Hct, %	pHb, g/dL	pH	P_{CO_2}, mmHg	HCO_3^-, mmol/L	P_{O_2}, mmHg	tHb, g/dL	S_{O_2}, %	K^+, mmol/L	Na^+, mmol/L	Ca^{2+}, mmol/L	Cl^-, mmol/L	Glu, mg/dL	Lac, mmol/L
BL														
LR	50±2	0.0±0.0	7.37±0.04	54.7±7.8	30.6±3.5	56.3±11.0	15.6±1.0	87.9±5.94	4.8±0.6	139±1	1.08±0.18	101±4	159±24	1.2±0.8
PEG500k	49±3	0.0±0.0	7.42±0.05	49.9±8.9	30.9±3.4	64.1±13.0	14.7±1.1	92.4±3.0	5.1±0.2	138±2$	1.17±0.12	100±4	181±48	1.7±0.7
PEG3500k	49±2	0.0±0.0	7.36±0.05	55.5±4.3	30.4±1.8	55.2±6.2	15.0±0.8	89.3±2.2	4.4±0.5	140±1	1.02±0.12	102±4	144±34	1.0±0.5
1 h														
LR	45±3†	0.1±0.0†	7.26±0.12	39.5±7.6†	16.8±2.4†#	99.1±7.6†@#	13.7±1.0†	96.6±1.3†#	4.1±0.4†	137±2	1.08±0.07	110±2†	160±30	4.1±0.9†#
PEG500k	46±3	0.0±0.0$	7.21±0.06†	47.0±5.6	18.6±3.7†	85.0±8.3†	13.3±0.9†	94.9±1.8†	3.8±0.3†	139±2	1.03±0.14	111±4†	148±44	3.1±1.3
PEG3500k	45±3	0.2±0.0†	7.27±0.03†	48.0±5.5	21.2±2.1†	74.7±7.1†	13.6±0.8	94.0±1.8†	3.9±0.2	139±2	0.95±0.12	109±4†	167±46	2.2±1.2†
2 h														
LR	43±3†	0.1±0.1	7.29±0.15	37.0±8.4†	17.1±2.3†#	103.9±6.8†@#	13.2±0.9†	97.6±0.9†@	4.0±0.5†	136±2†	1.05±0.06	111±2†	167±49	2.1±0.7@#
PEG500k	42±2†	0.0±0.0$	7.26±0.02†	44.1±6.0†	19.2±3.0†	87.5±6.9†	12.4±0.6†	96.2±0.9†	3.9±0.3†	138±2	1.05±0.11	112±4†	157±45	1.1±0.2
PEG3500k	41±4†	0.1±0.0†	7.30±0.04†	43.0±5.8†	20.7±2.9†	83.4±13.2†	12.9±1.0†	95.7±2.2†	4.0±0.4	138±1†	1.04±0.16	110±4†	133±30	0.8±0.4
24 h														
LR	33±3†	0.0±0.0	7.41±0.04	49.6±4.3	30.2±3.4	67.6±10.8	10.3±0.8†	93.5±2.8	4.8±0.2	140±1	1.20±0.08	104±3	163±28	2.2±1.3
PEG500k	34±2†	0.0±0.0	7.39±0.03	51.8±4.7	30.0±2.8	59.9±4.7	10.1±0.5†	92.0±2.3	4.8±0.4	140±1	1.27±0.21	101±4	147±35	3.1±1.1
PEG3500k	35±2†	0.0±0.0	7.41±0.01	54.9±3.2	33.4±1.9	66.9±3.1†	11.3±1.1†	93.4±0.8†	4.8±0.4	140±1	1.33±0.22†	99±2	175±24	1.9±0.8

$N = 6$ hamsters for all groups. The bicarbonate concentration was calculated based on the Henderson–Hasselbalch equation. BL, baseline; Glu, glucose; Hct, hematocrit; Lac, lactate; LR, lactated Ringer solution; P_{CO_2}, partial pressure of carbon dioxide; PEG, polyethylene glycol; PEG500k, PEG 500 kDa in LR; PEG3500k, PEG 3,500 kDa in LR; pHb, plasma hemoglobin; P_{O_2}, partial pressure of oxygen; S_{O_2}, hemoglobin saturation of oxygen; tHb, total hemoglobin. †$P < 0.05$ compared to BL, within each group. @$P < 0.05$, LR vs. PEG500k, at each time point. #$P < 0.05$, LR vs. PEG3500k, at each time point. $$P < 0.05$, PEG500k vs. PEG3500k, at each time point.

to BL values, apart from LR at 2 h after ECC and PEG3500k at 24 h after ECC. Venule S_{O_2} ($S_{V_{O_2}}$) showed more drastic changes compared to arterioles. Notably, $S_{V_{O_2}}$ in the PEG3500k group was significantly higher compared to both LR and PEG500k at 1 h and 2 h after ECC.
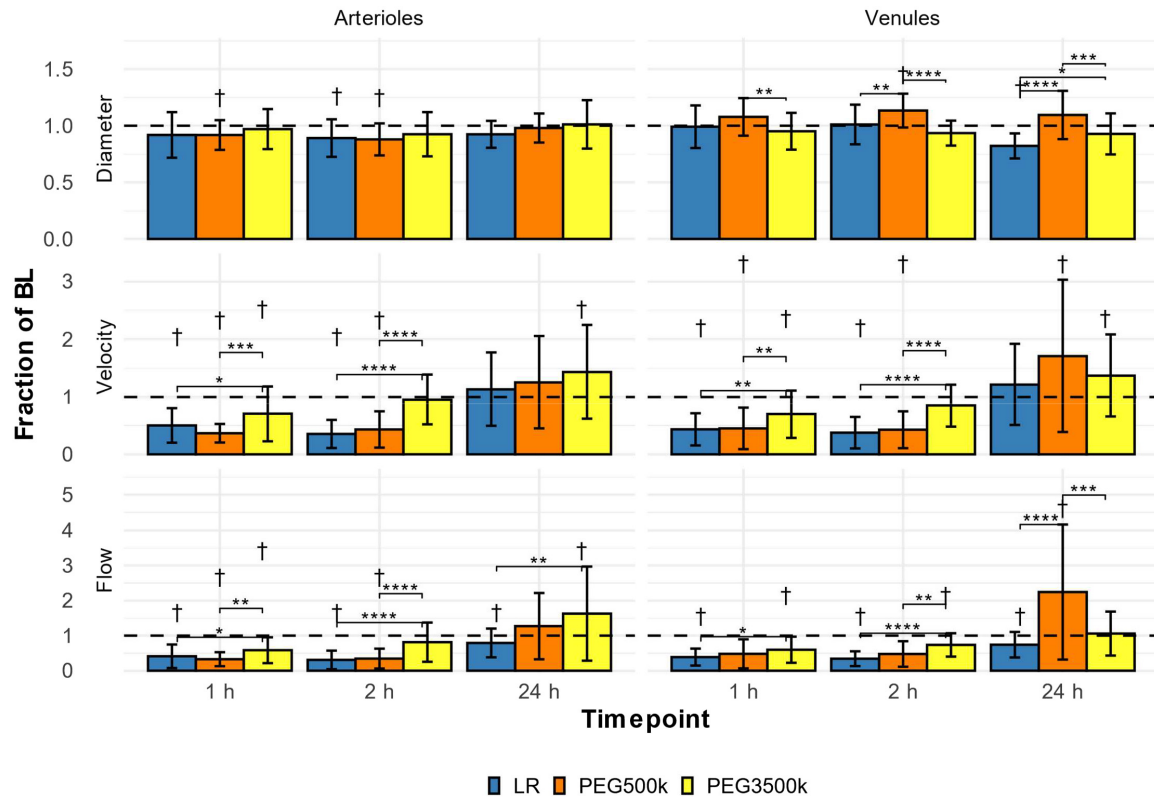
By averaging the flow and S_{O_2} for the arterioles and the venules for each animal at each time point, the oxygen delivery ($\dot{D}_{O_2}$), oxygen extraction ($\dot{V}_{O_2}$), and extraction ratio (O_2ER) were estimated by neglecting the O_2 dissolved in plasma (Table 2). Notably, the LR group was the only group that showed significant decrease in $\dot{D}_{O_2}$ compared to BL levels. At 1 h after ECC, the PEG3500k group showed a significant increase in both $\dot{D}_{O_2}$ and $\dot{V}_{O_2}$ compared to the PEG500k group but showed no significant difference compared to LR. The PEG3500k group at 2 h after ECC had significantly elevated $\dot{D}_{O_2}$ and $\dot{V}_{O_2}$ compared to the LR and PEG500k groups. No significant differences were observed at 24 h after ECC in $\dot{D}_{O_2}$, $\dot{V}_{O_2}$, or O_2ER.

Functional capillary density.

Functional capillary density (FCD) was adversely affected by the ECC procedure, as the FCD for all three groups was significantly lower at 1 and 2 h after ECC. However, at 24 h after ECC both PEG groups were able to recover close to BL values, whereas the LR control remained significantly lower than BL. Perhaps the most notable microvascular changes in this study were observed in FCD (Fig. 6) between the different groups. The FCD at 1 h after ECC dropped to an average of 41%, 53%, and 77% of BL levels for LR, PEG500k, and PEG3500k groups, respectively. At all post-ECC time points, the FCD for the PEG3500k group was significantly higher than that for both other groups.

Organ damage and inflammation.

The tissues excised at 24 h after ECC were analyzed by ELISA assays and flow cytometry techniques for markers of inflammation and damage (Table 3). None of the markers analyzed in any of the organs displayed significance between the two PEG groups at 24 h after ECC. The LR group was significantly elevated compared to the PEG3500k group for all cardiac markers of damage and inflammation. Almost all cardiac markers were significantly lower in the PEG500k group compared to the LR group, with the two exceptions being cardiac monocyte chemoattractant protein-1 (MCP-1) and IL-6. Renal interleukin-1 (IL-1), IL-6, and chemokine ligand 1 (CXCL1) were all significantly higher in LR compared to both PEG groups. The PEG3500k group was significantly lower than the LR group for serum creatinine, urinary creatinine, blood urea nitrogen (BUN), and IL-10. Urinary neutrophil gelatinase-associated lipocalin (u-NGAL) showed no difference between any of the groups. Serum alanine aminotransferase (AST) and aspartate aminotransferase (ALT), two markers of hepatic dysfunction, were significantly elevated in the LR group compared to both PEG groups at 24 h after ECC. Hepatic CXCL1 was significantly decreased in the PEG3500k group compared to the LR group. All markers of lung damage and inflammation were significantly lower in the PEG3500k group compared to the LR group. Serum fatty acid binding protein 2 (FABP2) and fatty acid binding protein 6 (FABP6) are two markers of small intestinal damage. Whereas FABP2 showed no significant difference between
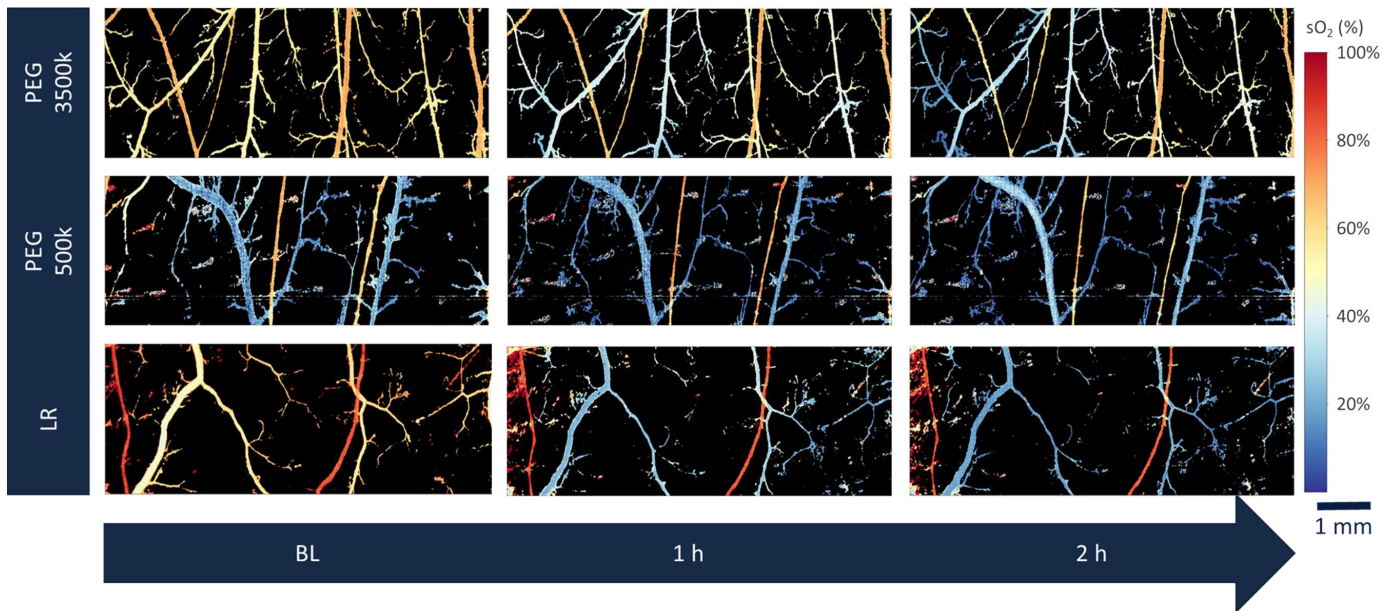
Figure 3. Changes in microvascular perfusion in arterioles (*left*) and venules (*right*) within the dorsal skinfold window chamber implanted into male Golden Syrian hamsters. From *top* to *bottom*: diameter, velocity, flow (calculated from diameter and velocity). Bar plots show means and SD. Data are normalized to baseline (BL) values, which are represented by the dashed lines. Lactated Ringer solution (LR) = blue; polyethylene glycol (PEG) 500 kDa in LR (PEG500k) = orange; PEG 3,500 kDa in LR (PEG3500k) = yellow. Baseline sample sizes for each group are arterioles: LR = 38, PEG500k = 34, PEG3500k = 58; venules: LR = 39, PEG500k = 35, PEG3500k = 44. Baseline arteriole values are as follows: *top*: LR = 63 µm, PEG500k = 63 µm, PEG3500k = 72 µm; *middle*: LR = 3.5 mm/s, PEG500k = 3.5 mm/s, PEG3500k = 3.9 mm/s; *bottom*: LR = 7 nL/s, PEG500k = 8 nL/s, PEG3500k = 13 nL/s. Baseline venule values are as follows: *top*: LR = 62 µm, PEG500k = 58 µm, PEG3500k = 63 µm; *middle*: LR = 0.8 mm/s, PEG500k = 0.7 mm/s, PEG3500k = 1.0 mm/s; *bottom*: LR = 1 nL/s, PEG500k = 1 nL/s, PEG3500k = 2 nL/s. †$P < 0.05$ compared to BL, within each group. *$P < 0.05$, **$P < 0.01$, ***$P < 0.001$, ****$P < 0.0001$ between groups, at each time point.

groups at 24 h, FABP6 was significantly elevated in the LR group compared to both PEG groups. Splenic CXCL1 was significantly elevated in the LR group compared to both PEG groups. In addition to markers of damage and inflammation, tissues were analyzed for markers of iron transport and sequestration. Serum bilirubin, serum ferritin, splenic ferritin, hepatic ferritin, renal ferritin, and cardiac ferritin were significantly elevated in the LR group compared to both PEG groups.

By using the leftover volume in the circuit after ECC, we were able to analyze serum at both 0 h and 24 h after ECC (Supplemental Table S3). Interestingly, all markers of renal, hepatic, and cardiac damage measured in the serum were significantly lower in the PEG3500k group compared to the PEG500k group at 0 h after ECC. Markers of small intestinal damage were significantly higher in the LR control group compared to the PEG3500k group at 0 h after ECC. Inflammatory markers at 0 h after ECC were consistently higher in the PEG500k group compared to the LR and PEG3500k groups. Ferritin levels in the LR group were significantly elevated compared to both PEG groups at 0 h after ECC. Although most markers showed a general increase between 0 and 24 h, bilirubin in the PEG3500k group decreased between 0 and 24 h.

DISCUSSION

The purpose of this study was to evaluate whether the addition of HMWLP to the crystalloid priming fluid of an ECC system improves microvascular perfusion and reduces the microvascular sequalae of ECC. Surprisingly, the PEG3500k group did not show much difference from BL values in arteriole or venule diameter at any time point after ECC. Velocity in both arterioles and venules was reduced in all groups at 1 h after ECC, but the PEG3500k group was the only group to recover back to BL by 2 h after ECC. Importantly, the PEG3500k group displayed a significant increase in arteriole and venule velocity compared to both other groups at 1 and 2 h after ECC. This comparison of velocity between groups was reflected in the calculated blood flow rate, suggesting that PEG3500k acutely improved microvascular perfusion after ECC primarily by increasing velocity. However, the most drastic change in microvascular perfusion was observed at the capillary level. At 1 h after ECC, the average FCD values after being normalized to BL were 41%, 53%, and 77% for LR, PEG500k, and PEG3500k groups, respectively. Furthermore, the PEG3500k group consistently showed a significant increase in FCD compared to the other two groups at all post-ECC time points.
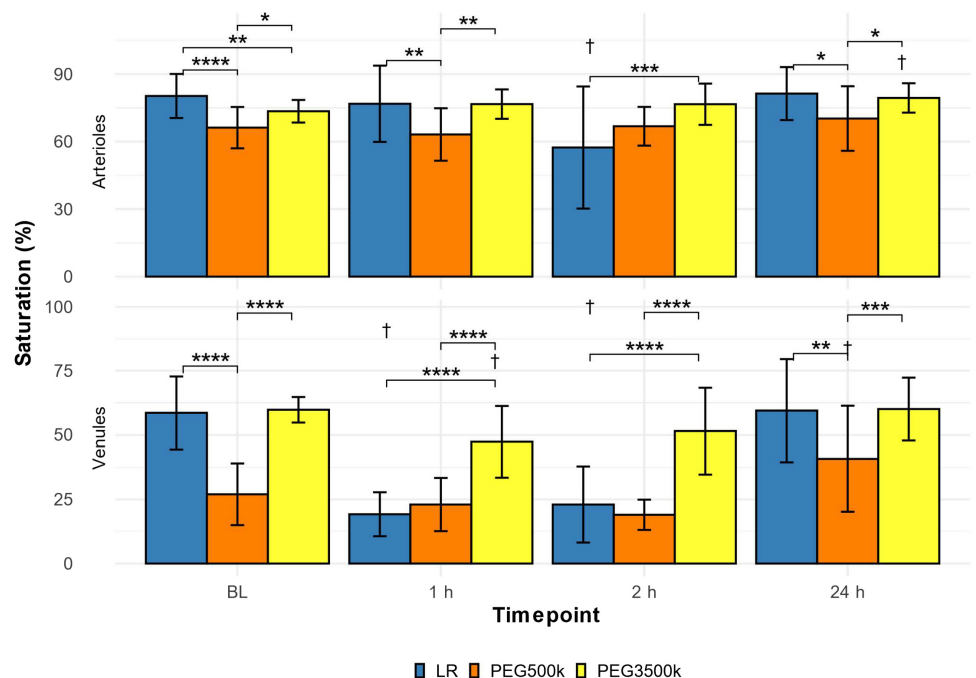
Figure 4. Representative hyperspectral images of oxygen saturation (So₂) of hemoglobin within the dorsal skinfold microcirculation preparation within the window chamber implanted into male Golden Syrian hamsters. From *top* to *bottom*: polyethylene glycol (PEG) 3,500 kDa in lactated Ringer solution (LR) (PEG3500k), PEG 500 kDa in LR (PEG500k), and LR. From *left* to *right*: baseline (BL), 1 h after extracorporeal circulation (ECC) (1 h), and 2 h after ECC (2 h). Color scale depicting saturation values is shown on *right*. Scale bar shown at *bottom right*.

As a result of increased FCD perfusion in the microcirculation, there is an impact on microvascular Hb O_2 saturation. Venule Hb O_2 saturation showed acute changes between the LR and PEG3500k groups. At BL, there were no significant differences between the two groups, but at 1 and 2 h after ECC, the PEG3500k group displayed significantly higher venule Hb oxygen saturation compared to the LR control group. In general, both PEG groups showed little change in venule Hb O_2 saturation from BL levels, whereas the LR group was significantly lower at both 1 and 2 h after ECC. Both PEG groups showed no significant decrease in arteriole Hb oxygen saturation from BL, and arteriole Hb oxygen saturation increased from BL levels at 24 h after ECC for the PEG3500k group. O_2 delivery, O_2 extraction, and the O_2 extraction ratio were estimated by using the average arteriole and venule perfusion and Hb oxygen saturation measurements. All groups experienced a drop in $\dot{D}O_2$, $\dot{V}O_2$, and O_2ER at 1 h after ECC compared to BL levels. However, the significantly increased $\dot{V}O_2$ and $\dot{D}O_2$ values for the PEG3500k group at 1 and 2 h after ECC compared to the LR and PEG500k groups suggest that the

Figure 5. Hemoglobin oxygen saturation within the dorsal skinfold microcirculation preparation within the window chamber implanted into male Golden Syrian hamsters. *Top*: arterioles. *Bottom*: venules. Bar plots show means and standard deviation. Baseline (BL) sample sizes for each group are arterioles: lactated Ringer solution (LR) = 21, polyethylene glycol (PEG) 500 kDa in LR (PEG500k) = 15, PEG 3,500 kDa in LR (PEG3500k) = 30; venules: LR = 24, PEG500k = 28, PEG3500k = 30. †$P < 0.05$ compared to BL, within each group. *$P < 0.05$, **$P < 0.01$, ***$P < 0.001$, ****$P < 0.0001$ between groups, at each time point.

Table 2. *Delivery of oxygen, oxygen extraction, and oxygen extraction ratio calculations*

|	$\dot{D}O_2$, nL O_2/s	$\dot{V}O_2$, nL O_2/s	O_2ER, %
BL			
LR	2.08 ± 0.99	1.73 ± 0.99	80 ± 12@
PEG500k	1.88 ± 0.94	1.77 ± 0.93	94 ± 4
PEG3500k	2.85 ± 1.15	2.75 ± 1.02	87 ± 6
1 h			
LR	0.78 ± 0.48	0.73 ± 0.48	89 ± 15
PEG500k	0.50 ± 0.40$	0.46 ± 0.40$	90 ± 8
PEG3500k	1.73 ± 0.83	1.55 ± 0.81	88 ± 10
2 h			
LR	0.39 ± 0.38†#	0.35 ± 0.37#	80 ± 19
PEG500k	0.46 ± 0.35$	0.42 ± 0.36$	90 ± 4
PEG3500k	2.11 ± 1.00	1.90 ± 0.94	90 ± 6
24 h			
LR	2.09 ± 1.09	1.96 ± 1.05	93 ± 3
PEG500k	1.89 ± 1.73	1.68 ± 1.66	87 ± 9
PEG3500k	3.28 ± 2.05	2.82 ± 2.19	77 ± 22

Note that these calculations were made by averaging saturations and blood flow rates for arterioles and venules separately. These calculations do not account for oxygen dissolved in plasma (this amount is negligible compared to the amount of oxygen bound by hemoglobin). BL, baseline; $\dot{D}O_2$, oxygen delivery; LR, lactated Ringer solution; O_2ER, oxygen extraction ratio; PEG, polyethylene glycol; PEG500k, (PEG) 500 kDa in LR; PEG3500k, PEG 3,500 kDa in LR; $\dot{V}O_2$, oxygen extraction. †$P < 0.05$ compared to BL within each group; @$P < 0.05$ between LR and PEG500k at each time point; #$P < 0.05$ between LR and PEG3500k at each time point; $$P < 0.05$ between PEG500k and PEG3500k at each time point.

addition of the PEG 3,500 kDa to LR helped improve O_2 delivery within the microvasculature and O_2 uptake by the surrounding tissue.

In addition to microvascular perfusion and oxygenation, the present study also analyzed markers of organ damage and inflammation. Apart from serum FABP2 and u-NGAL, all markers analyzed showed a significant decrease in the PEG3500k group compared to the LR control group at 24 h after ECC. On the other hand, no significant differences were observed between the two PEG groups in any of the markers analyzed at 24 h after ECC. However, marked differences

were observed between the two PEG groups when serum markers of organ damage were analyzed at 0 h after ECC. Serum AST and ALT, two markers of liver dysfunction, were elevated in the PEG500k group compared to the PEG3500k group. Renal dysfunction is one of the most common organ failures in ECMO; results show that serum creatinine and BUN were elevated in the PEG500k group compared to the PEG3500k group. Serum atrial natriuretic peptide (ANP), a marker of heart damage, was elevated in the PEG500k group compared to the PEG3500k group. Finally, serum markers of inflammation such as IL-6, IL-10, and CXCL1 were all significantly lower in the PEG3500k group compared to the PEG500k group. These results in tandem indicate that PEG3500k helps prevent organ damage and proinflammatory responses in ECC, which may improve patient outcomes in long-term ECC procedures such as ECMO.

Inflammatory responses are important to monitor during ECC procedures, since the circuit's surfaces are foreign and can alter coagulation and inflammation from blood contact. The use of ex vivo recirculation experiments helped confirm this by isolating the effects of the circuit contact and shear on blood. The increase in plasma hemoglobin (pHb) is primarily caused by the peristaltic pump used in the circuit, since shear stress surges as the tubing reaches complete occlusion. The dramatic drop in coagulation factors can primarily be explained by hemodilution from the priming fluids used, which also explains the changes in Hct and tHb. Whereas fibrinogen, soluble glycoprotein V, and platelet factor 4 were not significant between groups before ex vivo recirculation, the PEG500k group was statistically significantly higher than the PEG3500k and LR groups after ex vivo recirculation, suggesting that the addition of HMWLP aids in preserving the hemostatic balance. The most important results were the inflammation markers, since those increased after recirculation despite the hemodilution in all groups, confirming that inflammation results from the circuit contact itself. Additionally, IL-10 was lower in the PEG3500k group compared to the LR control group, demonstrating that the addition of HMWLP may reduce the response of the immune system to foreign surface contact.
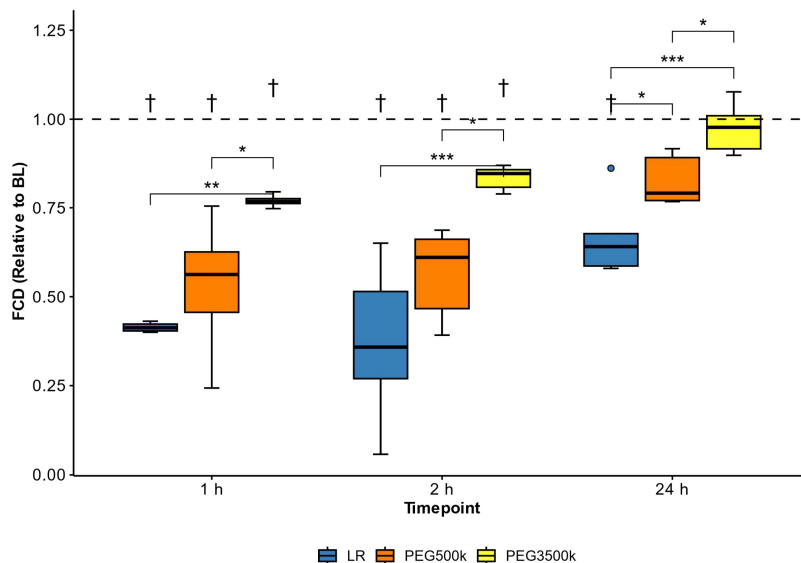
Figure 6. Functional capillary density (FCD) within the dorsal skinfold microcirculation preparation within the window chamber implanted into male Golden Syrian hamsters. Note that FCD is normalized to baseline (BL), which is represented by the dashed line. Data are presented as box-whisker plots displaying 25th percentile, median, and 75th percentile, along with minimum and maximum. Lactated Ringer solution (LR) = blue; polyethylene glycol (PEG) 500 kDa in LR (PEG500k) = orange; PEG 3,500 kDa in LR (PEG3500k) = yellow. Baseline median values are as follows: LR = 96, PEG500 = 97, PEG3500 = 112. †$P < 0.05$ compared to BL within each group. *$P < 0.05$, **$P < 0.01$, ***$P < 0.001$ between groups, at each time point.

Table 3. *Markers of organ damage and inflammation at 24 h after ECC*

Heart

Group	Ferritin, µg/g protein	CXCL1, pg/mg protein	IL-6, pg/mg protein	IL-10, pg/mg protein	IL-1, pg/mg protein	Troponin, ng/mL	CRP, ng/mg	TNF-α, pg/mg protein	MCP-1, pg/mg protein	Serum ANP, ng/mL
LR	732±217@#	102±44@#	302±128#	155±66@#	83±36@#	322±85@#	1,064±438@#	370±145@#	292±134#	1.6±0.7@#
PEG500k	443±53	64±6	195±11	95±14	46±6	232±35	617±73	221±25	177±24	1.0±0.1
PEG3500k	420±98	49±6	162±21	75±7	38±4	211±28	475±38	182±23	141±17	0.9±0.1

Kidney

Group	Ferritin, µg/g protein	CXCL1, pg/mg protein	IL-6, pg/mg protein	IL-10, pg/mg protein	IL-1, pg/mg protein	Serum creatinine, mg/dL	BUN, mg/dL	u-NGAL, ng/dL	Urinary creatinine, mg/dL
LR	624±148@#	227±98@#	420±183@#	224±103@#	228±95@#	3.9±1.3#	2.8±1.0#	1,639±923	1.7±0.6#
PEG500k	426±66	128±17	255±27	137±11	130±13	2.9±0.5	2.0±0.4	1,136±146	1.4±0.2
PEG3500k	405±74	97±12	211±22	104±11	113±7	2.5±0.3	1.8±0.1	1,021±93	1.1±0.1

Serum / **Lung**

Group	Ferritin, µg/mL	CXCL1, pg/mL	IL-6, pg/mL	IL-10, pg/mL	Bilirubin, mg/dL	Epi, pg/mL	Nor-Epi, pg/mL	CXCL1, pg/mg protein	MPO	Neu +
LR	531±146@#	646±194@#	670±207#	530±208@#	6.1±2.5@#	560±141	709±219#	297±125#	266±81#	90±41#
PEG500k	373±40	413±37	483±72	290±43	3.6±0.4	464±73	503±88	209±24	196±28	70±7
PEG3500k	359±29	366±16	433±42	267±24	3.2±0.2	438±28	444±55	165±24	160±26	49±9

Liver / **Spleen** / **Small Intestine**

Group	Ferritin, µg/g protein	CXCL1, pg/mg protein	AST, u/L	ALT, u/L	Ferritin, µg/g protein	CXCL1, pg/mg protein	FABP2, pg/mL	FABP6, pg/mL
LR	1,795±343@#	659±276#	88±26@#	79±28#	568±255@#	986±407@#	1,562±318	2,223±963@#
PEG500k	1,381±96	454±42	60±8	44±2	306±50	608±76	1,290±178	1,164±120
PEG3500k	1,270±161	347±51	54±3	42±3	255±26	488±28	1,308±49	1,087±59

Data are displayed as means ± SD. $N = 6$ hamsters for all groups. ALT, alanine transferase; ANP, atrial natriuretic peptide; AST, aspartate transferase; BUN, blood urea nitrogen; CRP, C-reactive protein; CXCL1, C-X-C motif chemokine ligand 1; ECC, extracorporeal circulation; Epi, epinephrine; FABP2, fatty acid binding protein 2; FABP6, fatty acid binding protein 6; IL, interleukin; LR, lacted Ringer solution; MCP, monocyte chemoattractant protein-1; MPO, myeloperoxidase; Neu +, neutrophil count; Nor-Epi, norepinephrine; PEG, polyethylene glycol; PEG500k, PEG 500 kDa in LR; PEG3500k, PEG 3,500 kDa in LR; TNF, tumor necrosis factor; u-NGAL, urinary neutrophil gelatinase-associated lipocalin. @$P < 0.05$, LR vs. PEG500k; #$P < 0.05$, LR vs. PEG3500k.

Although the present results seem to indicate that there are a multitude of benefits, there are several limitations. First, the present study only used male Golden Syrian hamsters, so further studies are required to determine the impact of biological sex on the efficacy of using HMWLPs during VA-ECC. Second, the flow rates in the present study are much lower than those used in a clinical setting for VA-ECMO or CPB. We attribute this to the fact that we used a small-rodent model, with the weight being ~1,000 times lower and the resting HR being between 6–8 times higher than a typical adult human. Third, it needs to be noted that the hemodynamics of the circuit used in the present study are not representative of the clinical setting. Currently, most institutions have chosen to use centrifugal pumps to drive blood flow through the circuit. Unlike the pulsatory roller pump, centrifugal pumps usually flow continuously and may introduce some turbulence into the circuit. Both these conditions may affect the efficacy of HMWLP in a clinical application, and therefore further testing on a centrifugal pump system is warranted to determine the HMWLP's effect on RBC lysis. Fourth, the ELISA assays used for organ analysis utilized commercial kits intended for use with rats and/or human samples. Although the actual numeric values were not assessed for accuracy, precision was ensured, as all samples were run with the same kits and followed manufacturer-suggested procedures and all samples for the PEG500k and PEG3500k groups were run on the same plate. Finally, this study utilized a dorsal window chamber model, which cannot predict the changes in microvascular flow in other areas of the body that may be sensitive to ECC. However, our previous studies have indicated a good correlation between the hemodynamics of the dorsal window and vital organs (32).

Conclusions

The present study provides a starting point for research into the potential benefits of using high-molecular-weight linear polymers (HMWLPs) in priming fluids for ECC procedures. A 5 ppm solution of PEG500k or PEG3500k HMWLP was mixed into LR and used to prime a scaled-down circuit of venoarterial ECC. Results show a substantial increase in velocity for arterioles and venules in the PEG3500k group compared to the LR control and PEG500k groups, as well as a significant increase in the perfusion of capillaries with RBCs. Additionally, reductions in markers of inflammation and damage were observed in the PEG3500k group immediately after ECC in key organs such as the liver, kidney, and heart compared to both other groups. Future work is required to determine feasibility when used in a centrifugal pump system and optimize HMWLP parameters such as type, molecular weight, and concentration.

DATA AVAILABILITY

Data will be made available upon reasonable request.

SUPPLEMENTAL MATERIAL

Supplemental Tables S1–S3: https://doi.org/10.6084/m9.figshare.c.6675536.v1.

ACKNOWLEDGMENTS

DISCLOSURES

No conflicts of interest, financial or otherwise, are declared by the authors.

AUTHOR CONTRIBUTIONS

K.G. and P.C. conceived and designed research; K.G. and C.W. performed experiments; K.G. analyzed data; K.G. and P.C. interpreted results of experiments; K.G. prepared figures; K.G. drafted manuscript; K.G. and P.C. edited and revised manuscript; K.G. and P.C. approved final version of manuscript.

REFERENCES

1. **Toms B.** Some observations on the flow of linear polymer solutions through straight tubes at large Reynolds numbers. 1948. https://www.semanticscholar.org/paper/Some-Observations-on-the-Flow-of-Linear-Polymer-at-Toms/ded20d3df4a763b7212e0047a0c604ff867f8a58 [2022 Jun 21].

2. **Virk PS, Merrill EW, Mickley HS, Smith KA, Mollo-Christensen EL.** The Toms phenomenon: turbulent pipe flow of dilute polymer solutions. *J Fluid Mech* 30: 305–328, 1967. doi:10.1017/S0022112067001442.

3. **Kameneva MV.** Microrheological effects of drag-reducing polymers in vitro and in vivo. *Int J Eng Sci* 59: 168–183, 2012. doi:10.1016/j.ijengsci.2012.03.014.

4. **White CM, Mungal MG.** Mechanics and prediction of turbulent drag reduction with polymer additives. *Annu Rev Fluid Mech* 40: 235–256, 2008. doi:10.1146/annurev.fluid.40.111406.102156.

5. **Pereira AS, Mompean G, Thais L, Thompson RL.** Statistics and tensor analysis of polymer coil–stretch mechanism in turbulent drag reducing channel flow. *J Fluid Mech* 824: 135–173, 2017. doi:10.1017/jfm.2017.332.

6. **Benzi R, Ching ES.** Polymers in fluid flows. *Annu Rev Condens Matter Phys* 9: 163–181, 2018. doi:10.1146/annurev-conmatphys-033117-053913.

7. **Burger ED, Chorn LG, Perkins TK.** Studies of drag reduction conducted over a broad range of pipeline conditions when flowing prudhoe bay crude oil. *J Rheol* 24: 603–626, 1980. doi:10.1122/1.549579.

8. **Burger ED, Munk WR, Wahl HA.** Flow increase in the Trans Alaska pipeline through use of a polymeric drag-reducing additive. *J Pet Technol* 34: 377–386, 1982. doi:10.2118/9419-PA.

9. **Mostardi RA, Greene HL, Nokes RF, Thomas LC, Lue T.** The effect of drag reducing agents on stenotic flow disturbances in dogs. *Biorheology* 13: 137–141, 1976. doi:10.3233/BIR-1976-13208.

10. **Mostardi RA, Thomas LC, Greene HL, VanEssen F, Nokes RF.** Suppression of atherosclerosis in rabbits using drag reducing polymers. *Biorheology* 15: 1–14, 1978.

11. **Greene HL, Mostardi RF, Nokes RF.** Effects of drag reducing polymers on initiation of atherosclerosis. *Polym Eng Sci* 20: 499–504, 1980. doi:10.1002/pen.760200710.

12. **Kameneva MV, Wu ZJ, Uraysh A, Repko B, Litwak KN, Billiar TR, Fink MP, Simmons RL, Griffith BP, Borovetz HS.** Blood soluble drag-reducing polymers prevent lethality from hemorrhagic shock in acute animal experiments. *Biorheology* 41: 53–64, 2004.

13. **Bragin DE, Kameneva MV, Bragina OA, Thomson S, Statom GL, Lara DA, Yang Y, Nemoto EM.** Rheological effects of drag-reducing polymers improve cerebral blood flow and oxygenation after traumatic brain injury in rats. *J Cereb Blood Flow Metab* 37: 762–775, 2017. doi:10.1177/0271678X16684153.

14. **Bragin DE, Lara DA, Bragina OA, Kameneva MV, Nemoto EM.** Resuscitation fluid with drag reducing polymer enhances cerebral microcirculation and tissue oxygenation after traumatic brain injury complicated by hemorrhagic shock. *Adv Exp Med Biol* 1072: 39–43, 2018. doi:10.1007/978-3-319-91287-5_7.

15. **Crompton D, Vats R, Pradhan-Sundd T, Sundd P, Kameneva MV.** Drag-reducing polymers improve hepatic vaso-occlusion in SCD mice. *Blood Adv* 4: 4333–4336, 2020. doi:10.1182/bloodadvances.2020002779.

16. **Hu F, Zha D, Du R, Chen X, Zhou B, Xiu J, Bin J, Liu Y.** Improvement of the microcirculation in the acute ischemic rat limb during intravenous infusion of drag-reducing polymers. *Biorheology* 48: 149–159, 2011. doi:10.3233/BIR-2011-0592.

17. **Tohme S, Kameneva MV, Yazdani HO, Sud V, Goswami J, Loughran P, Huang H, Simmons RL, Tsung A.** Drag reducing polymers decrease hepatic injury and metastases after liver ischemia-reperfusion. *Oncotarget* 8: 59854–59866, 2017. doi:10.18632/oncotarget.18322.

18. **Kameneva MV, Polyakova MS, Fedoseeva EV.** Effect of drag-reducing polymers on the structure of the stagnant zones and eddies in models of constricted and branching blood vessels. *Fluid Dyn* 25: 956–959, 1990. doi:10.1007/BF01049712.

19. **Pacella JJ, Kameneva MV, Brands J, Lipowsky HH, Vink H, Lavery LL, Villanueva FS.** Modulation of pre-capillary arteriolar pressure with drag-reducing polymers: a novel method for enhancing microvascular perfusion. *Microcirculation* 19: 580–585, 2012. doi:10.1111/j.1549-8719.2012.00190.x.

20. **Marhefka JN, Zhao R, Wu ZJ, Velankar SS, Antaki JF, Kameneva MV.** Drag reducing polymers improve tissue perfusion via modification of the RBC traffic in microvessels. *Biorheology* 46: 281–292, 2009. doi:10.3233/BIR-2009-0543.

21. **Li G, Sun Y, Zheng X, Choi HJ, Zhang K.** Effect of drag-reducing polymer on blood flow in microchannels. *Colloids Surf B Biointerfaces* 209: 112212, 2022. doi:10.1016/j.colsurfb.2021.112212.

22. **Secomb TW.** Blood flow in the microcirculation. *Annu Rev Fluid Mech* 49: 443–461, 2017. doi:10.1146/annurev-fluid-010816-060302.

23. **Battiato I, Tartakovsky D, Cabrales P, Intaglietta M.** Role of glycocalyx in attenuation of shear stress on endothelial cells: from in vivo experiments to microfluidic circuits. *2017 European Conference on Circuit Theory and Design (ECCTD)*. 2017, 1–4. doi:10.1109/ECCTD.2017.8093276.

24. **Brands J, Kliner D, Lipowsky HH, Kameneva MV, Villanueva FS, Pacella JJ.** New insights into the microvascular mechanisms of drag reducing polymers: effect on the cell-free layer. *PLoS One* 8: e77252, 2013. doi:10.1371/journal.pone.0077252.

25. **Govender K, Jani VP, Cabrales P.** The disconnect between extracorporeal circulation and the microcirculation: a review. *ASAIO J* 68: 881–889, 2022. doi:10.1097/MAT.0000000000001618.

26. **Govender K, Cabrales P.** Extracorporeal circulation impairs microcirculation perfusion and organ function. *J Appl Physiol (1985)* 132: 794–810, 2022. doi:10.1152/japplphysiol.00726.2021.

27. **Cabrales P, Acero C, Intaglietta M, Tsai AG.** Measurement of the cardiac output in small animals by thermodilution. *Microvasc Res* 66: 77–82, 2003. doi:10.1016/S0026-2862(03)00044-X.

28. **Wayland H, Johnson PC.** Erythrocyte velocity measurement in microvessels by a two-slit photometric method. *J Appl Physiol* 22: 333–337, 1967. doi:10.1152/jappl.1967.22.2.333.

29. **Intaglietta M, Tompkins WR.** Microvascular measurements by video image shearing and splitting. *Microvasc Res* 5: 309–312, 1973. doi:10.1016/0026-2862(73)90042-3.

30. **Lipowsky HH, Firrell JC.** Microvascular hemodynamics during systemic hemodilution and hemoconcentration. *Am J Physiol Heart Circ Physiol* 250: H908–H922, 1986. doi:10.1152/ajpheart.1986.250.6.H908.

31. **Lucas A, Ao-leong ES, Williams AT, Jani VP, Muller CR, Yalcin O, Cabrales P.** Increased hemoglobin oxygen affinity with 5-hydroxymethylfurfural supports cardiac function during severe hypoxia. *Front Physiol* 10: 1350, 2019. doi:10.3389/fphys.2019.01350.

32. **Cabrales P, Tsai AG.** Plasma viscosity regulates systemic and microvascular perfusion during acute extreme anemic conditions. *Am J Physiol Heart Circ Physiol* 291: H2445–H2452, 2006. doi:10.1152/ajpheart.00394.2006.